Advanced Modelling Techniques for Flexible Robotic Systems

Mariapaola D'Imperio[1(✉)], Cristiano Pizzamiglio[2], Daniele Ludovico[2],
Darwin G. Caldwell[1], Giancarlo Genta[2], and Ferdinando Cannella[1]

[1] ADVR, Istituto Italiano di Tecnologia, Genova, Italy
{mariapaola.dimperio,darwin.caldwell,ferdinando.cannella}@iit.it
[2] DIMEAS, Politecnico di Torino, Torino, Italy
{cristiano.pizzamiglio,giancarlo.genta}@polito.it,
daniele.ludovico@studenti.polito.it

Abstract. The purpose of this paper is to present a 3 DoF under-actuated mechanism with one flexible component. It is called FLEGX (FLEXible LEG) and it would be the first step in the design of a jumping humanoid robot with flexible limbs. An early system-level design validation of the FLEGX mechanical configuration was performed using the software MSC.Nastran® and MSC.Adams®-Matlab/Simulink® integrated environment.

Keywords: Flexible robotic leg · Multi-body analysis · Jumping robot

1 Introduction

Robotics is the *branch of mechanical engineering, electrical engineering and computer science that deals with the design, construction and operation of robots.* Even if the first automatic machines can be traced back to Leonardo da Vinci robotics can be defined a quite recent discipline due to the fact that its first "official" apparition was in 1942 when I. Asimov wrote the *Three Laws of Robotics* followed by the principles of cybernetics written by N. Wiener in the 1948. The first programmable robot appeared in 1961, it is called Ultimate and it was designed to manipulate hot metal components [1]. Jumping over the decades, the robotic world has made incredible progresses: an example of how far it has been moved from the first steps was brought on stage in the last of Darpa robotics challenges, hosted in May 2015 [2].

There are many different subcategories afferent to robotics, their classification depends on the target field, as for example: biomedical robotics, humanoids robotics, legged systems robotics, etc. Each of them requires a perfect integration among electronics, mechanics and control to achieve the best results ever. In particular, while remaining important the role played by electronics, as soon as the robots dimension or the complexity of the interaction with the external world increases, the integration between mechanics and control becomes more and more important since the early stage of its development process.

Massive and bulky robots generate high forces in the interaction with the external environment that can damage their structures or can create unwanted feedback for the control system [4]. Those actions increase with the rise of the dynamic capabilities of such machines, in fact for example, in a running legged robot, the ground reaction force registered on the limbs can reach 2.5 times its total weight [5]. In the other side, thinking to the biomedical robots or the manipulators that have to interact with humans, the forces exerted from the interaction can damage the counterpart. Watching closer at this human robotic interaction, it has to be considered that in the near future the humans that interact with robots are not only the trained workers of an assembly line but also common people, not trained, which will use a robot at their home [6].

If those robots are conceived as flexible, their structure becomes lighter and more compliant, that results in faster and safer robotic systems. When the structural flexibility is taken into account, in fact, the aforementioned integrated approach permits not only to deeply consider the relationship between structural capabilities and control algorithm requests, but also to exploit the optimal solutions in terms of energy consumption. However, the design and optimization of a compliant mechanism, is a challenging task especially when the flexible structure undergoes large deflections [7].

Following the same research line of other works of the same authors [8,9], in this paper the development process of an articulated FLEXible LEG (called FLEGX), based on the Virtual Prototyping Design techniques, is presented. The understanding of the overall system performances as a function of the flexibility is of key importance and requires a vast simulation campaign. However, studying tens of geometrically different flexible links interfacing a Finite Element software and a large displacement multibody software would be too time consuming [10]. For these reasons, a hierarchical approach has been used in the design process here presented, with the aim of preventing misleading results especially at the initial stage when few data were available. Several solutions, detailed in the following paragraphs, were investigated by means of three different Virtual Models such as Pseudo-Rigid Model (PRBM), Linear Flexible model (LFM) and Machinery Model (MM) in order to achieve FLEGX optimal design.

The rest of the paper is organized as follows. Section 2 describes the mechanism, Sect. 3 details the performance analysis while in Sect. 4 conclusions and the future works will be illustrated.

2   Mechanism Description

The aim of this section is to describe the four different FLEGX mechanical solutions designed before reaching the optimal one. FLEGX (Fig. 1.I) is a 3 DoF underactuated mechanism, in which both the hip and knee joints are actuated, whereas the translational joint is not. As previously stated, the novelty of this robotic leg lies in making flexible the lower link of the structure; on the contrary, the upper segment is rigid. The numerical simulation campaigns, carried out during the design process, allowed to investigate the advantages and drawbacks
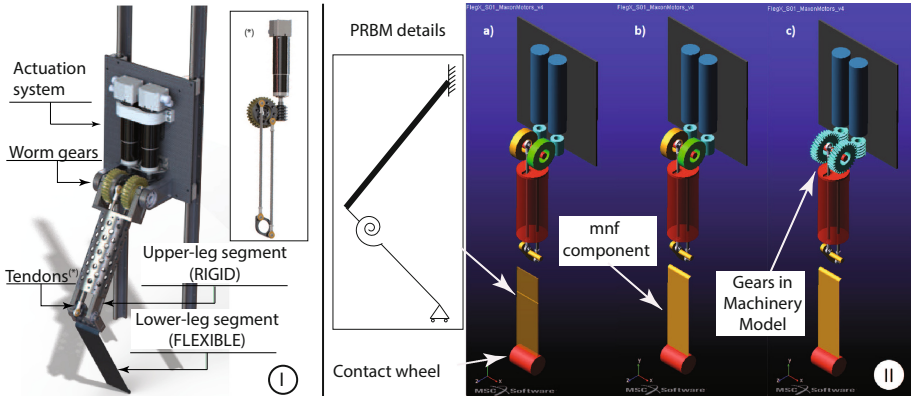
Fig. 1. (I) FLEGX schema No. 4 and details, (II) Numerical Models: (a) Pseudo-Rigid-Body; (b) Linear Flexible; (c) Machinery.

of the different mechanical concepts and eventually to select the configuration that satisfactorily met the performance requirements in terms i.e. of jump height.

In **Solution No. 1** the upper link structure is similar to the HyQ's [12] upper leg segment, namely it consists of two parallel steel plates linked together by means of two horizontal steel rods. The two brushless electric motors (and their gearheads) are directly coupled to the hip and knee joints. This is a very simple and reliable mechanical configuration with the drawback of having heavy rigid segment and, as consequence, lower system dynamic performances (Table 2).

In **Solution No. 2**, instead, the upper leg segment consists of a commercial round aluminium tube having a 90 mm outer diameter. Both the brushless DC motors and gearheads are placed close to the hip joint with their longitudinal axis parallel to the one of the upper leg cylinder. In order to transmit the motion, a couple of bevel gears is used at the hip joint, whereas a combination of a couple of bevel gears and a toothed belt is employed at the knee joint. This solution presents high torsional stiffness of the upper leg segment due to its circular section, but, at the same time, it has a low efficiency due to the consistent mechanical complexity, low system reliability and heavy weight (Table 2).

In the configuration of **Solution No. 3**, the rigid segment features an aircraft semi-monocoque fuselage-like structure. The hip joint brushless DC motor is placed directly on the linear guide support plate, whereas the knee joint actuator is mounted within the upper leg structure. With the aim of reducing the loads acting on the actuators during the jumping and landing phases, worm drives, with a 50:1 gear ratio, are employed for the transmission of the motion at both joints. In this solution, a very high torsional and axial stiffness of the upper leg segment and very low mass of the rigid segment are achieved (Table 2). However its construction would require higher costs and would take longer time due to the fact that the rigid link parts aren't commercial components.

The biologically inspired version of the FLEGX system, **Solution No. 4** (Fig. 1.I), adopts both the relevant features of the solutions No. 2 and No. 3 and also new ones. The whole actuation system is directly mounted on the linear guide support plate, hence reducing the mass and the moments of inertia of the rigid segment. Even for this configuration, worm drives are used, but with a 9.67:1 gear ratio. In order to transmit the motion at the knee joint, a floating worm wheel is employed: the hole of the wheel is drilled out allowing a deep groove double row ball bearing to be coupled with it; in turn, the inner ring of the ball bearing is constrained to the hip joint shaft, resulting in decoupling the motion of the hip and knee worm wheels. Eventually, a tendon-like system transfers the motion from the worm wheel to the knee joint. The two 266 mm-long tendons are steel rods having a diameter of 7 mm and a 10 mm-long thread at both ends. The tendons are linked to the worm gear and to the knee joint flange by means of spherical bearings (Fig. 1.I) (Table 1).

Table 1. Mass and central moments of inertia of the most important components of the configuration No. 4.

Component/ Subsystem	Mass [kg]	Central moments of inertia $[kg \cdot m^2]$		
		I_{xx}	I_{yy}	I_{zz}
Linear guide (with Motors and Gearheads)	5.1920	$1.6462 \cdot 10^{-2}$	$4.1510 \cdot 10^{-2}$	$5.3333 \cdot 10^{-2}$
Upper leg segment	0.8567	$1.1990 \cdot 10^{-3}$	$9.5590 \cdot 10^{-3}$	$1.0204 \cdot 10^{-2}$
Worm	0.1843	$3 \cdot 10^{-5}$	$4 \cdot 10^{-5}$	$4 \cdot 10^{-5}$
Worm gear	0.5008	$2.5500 \cdot 10^{-4}$	$2.5500 \cdot 10^{-4}$	$4.8100 \cdot 10^{-4}$
Flexible link (L = 250 mm, W = 70 mm, t = 3 mm)	0.4598	$1.9300 \cdot 10^{-4}$	$2.8680 \cdot 10^{-3}$	$3.0510 \cdot 10^{-3}$

As in the Solution No. 2, the upper leg segment consists of a commercial round thin-wall aluminum tube having an outer diameter of 75 mm, inner diameter equal to 71 mm and a length of 180 mm. The round tube features several holes with the purpose of lightening the structure: its resulting mass is equal to 165g. Despite the high mass of the linear subsystem this solution presents a good torsional/axial stiffness and low mass (Table 2) and moments of inertia of the rigid segment and, in addition, the advantage of being composed by several commercial parts.

Each of the aforementioned solutions was investigated by means of three different Virtual Model following a hierarchical process as stated before. The first one was a Pseudo-Rigid-Body model (PRBM) [11] (Fig. 1.II.a). In this model the flexibility was lumped in a spring element having a proper stiffness coefficient. It results in a very fast system that permitted to have an idea of the allowable system jumping height. Subsequently in the LFM, thanks to the introduction of a linear flexible component in the multibody model, more accurate analysis

were performed (Fig. 1.II.b). In this case, the flexible component was modelled as a modal neutral file and the maximum Von Mises stresses were evaluated. The most complicated model was the MM one, it was designed by using the MSC.Adams/Machinery® module, and thanks to it a number of analyses were carried out adding to the model detailed virtual prototypes of the hip/knee worm drives in order to assess the influence of the efficiency of the latter on the FLEGX performance (Fig. 1.II.c).

3   Performance Analysis

The numerical analyses of the robotic leg were performed paying particular attention to deformations and stresses of the flexible link developed during take-off and landing phases of a jump movement; for these reasons, in this section, the results of the LFM during the take-off stage were described.

   As stated before, in the LFM, the flexible component was integrated in a multi-body environment by means of a modal neutral file (mnf). This file, generated with a Finite Element software, contains information such as inertia matrix invariants, mode-shapes and frequencies of the modal base derived from fixed boundary eigenmodes through an orthonormalization procedure.

   The simulations were performed by requiring that the maximum flexible link stresses were lower than the ultimate tensile strength of the link material, namely between 510 and 530 MPa (Von Mises criterion). The jumping technique (i.e. countermovement jump) applied to the four mechanical configurations can be described as follows: the robotic leg starts at a static standing position and then squats down, in three seconds, by a 55 degrees clockwise and counterclockwise rotation, with respect to the vertical axis, of the hip and knee joints respectively; eventually, at $t = 3s$ the hip and knee joints rapidly rotate again, but in the opposite directions, allowing the leg to jump vertically up off the ground.

   The rotations at the hip and knee joints were dictated by motion laws as a function of time. These joint motions feature a combination of STEP functions which approximate the Heaviside step function with a cubic polynomial. The STEP function has continuous first derivative and a discontinuous second derivative at $t = t_i$ (initial time) and $t = t_f$ (final time). For instance, the hip motion law is the following:

$$step(time, 0, 0, 3, 55d) - step(time, 3, 0, 3 + Dt, 55d)$$

where Dt is a design variable representing the time interval, whose value lies between 0.40 and 0.45s, during which the final jumping stage occurs.

   The mass of the group consisting of motor and gearhead was assumed to be equal to 2.2 kg for each of the two joints. At this stage, no assumptions were made about the motors and gearheads performance. With the aim of reducing the solution time and avoiding solver issues during the simulations, the contact between the flexible link and the ground was not directly modelled, but the interaction between the ground and a negligible mass rigid cylinder (Fig. 1.II), constrained by a fixed joint to the lower interface node of the flexible link,

Table 2. Theoretical jump heights of the four mechanical concepts.

Configuration	Total mass [kg]	Jump height [mm]	Max. stress [MPa](VonMises)
No. 1	8.77	70.88	522.90
No. 2	9.57	59.80	523.62
No. 3	7.35	108.1	514.62
No. 4	7.97	104.1	530.68

was implemented. That choice permitted to model the contact between two rigid bodies by using the Impact-Function-Based function that implements a nonlinear spring damper element.

The simulations were run using the *GSTIFF* implicit predictor - corrector integrator and, with the aim of increasing the stability and robustness of the solver, the *SI2* (Stabilized Index 2) formulation was used. Usually, the *SI2* allows to avoid the very short-duration numerical spikes for velocities and accelerations. After several preliminary simulations the permissible solution convergence error was set to $1 \cdot 10^{-4}$. Jump heights, maximum stresses developed in the flexible link and total mass, defined in the multibody software, of the mechanical concepts are reported in Table 2. It may be observed that the solutions No. 3 and No. 4 shown the best performances with a jump height of 108.1 and 104.1 mm respectively. Taking into account the observations made in the previous section, the solution No. 4 was the selected one.

4   Results and Conclusions

In this paper the design of an articulated 3DoF underactuated flexible robotic leg has been presented. The system performances have been tested by means of a fruitful campaign of multibody simulations performed by MSC.Nastran® and MSC.Adams®-Matlab/Simulink® integrated environment. That choice permitted to choose the optimal solutions in terms of robot weight and jumping performances (Table 2).

In Fig. 2 are shown the results of a take-off and landing numerical analysis of the selected mechanical configuration (Solution No. 4) considering three different modelling techniques for the lower link: rigid, PRBM and linear flexible. The simulations were carried out assuming a jump height approximately equal to 50 mm and considering a 250 mm long, 70 mm wide and 3 mm thick link. It may be noticed that the flexible link guarantees a lower requirement in terms of hip and knee torques with respect to the rigid one. Moreover, the PRBM approximates quite well the behavior of the linear flexible link based on the Component Mode Synthesis techniques.

In conclusion, simulations of the Solution No. 4 were performed including in the model both the linear flexible link and virtual prototypes of the worm gears employing the 3D Contact algorithm, which is a geometry-based contact method; in general, worm gears have low efficiencies, hence their impact on the overall performance of the robotic leg was evaluated as displayed in Fig. 3.
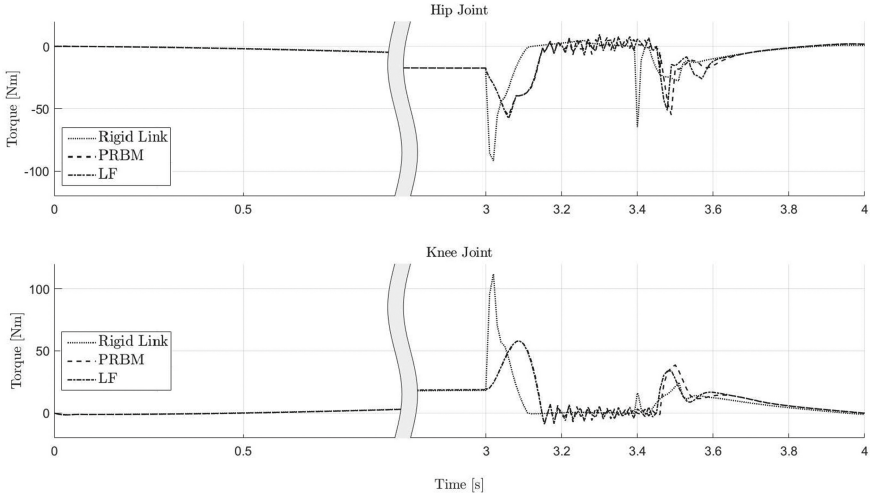
Fig. 2. Take-off and landing analysis of the Solution No. 4. The results show the torque values at the hip and knee joints for three different modelling solutions of the link. The graph is cutted in order to highlight both the preparatory phase and the jumping one.
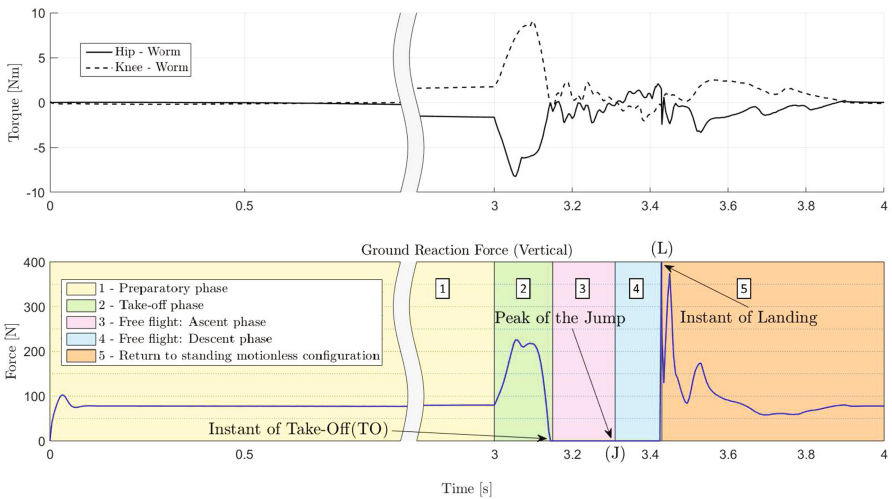

Fig. 3. Detailed numerical analysis of the configuration No. 4 with the linear flexible link and virtual worm gears. The take-off and landing phases were simulated imposing a maximum vertical jump height equal to 50 mm and assuming a 64% efficient worm gears. The jumping strategy is similar to the one previously described in Sect. 3. The upper plot shows the values of the torque for the hip and knee worms, whereas the lower plot illustrates the evolution of the vertical component of the ground reaction force. The point (J) represents the moment when the center of mass of the robotic leg is at rest and at its higher vertical position. The graph is cutted in order to highlight both the preparatory phase and the jumping one.

Future works concern the implementation, in the Virtual Model, of a nonlinear flexible link based on implicit nonlinear Finite Element Analysis, the development of the physical prototype and the accomplishment of an extended campaign of experimental test to collect data useful for the numerical model validation. At the same time, the control system will be developed. It will consists in a double layer schema: the low level and the high level respectively. The low level is based on the singular perturbation theory applied to a hybrid system to obtain an order reduction model. The high level control, instead, is based on the theory of hybrid system. Its aim is to produce a stable orbit in the state space variable in order to obtain a controlled sequence of jumps.

References

1. Malone R (2004) Ultimate robot. DK Publishing, London
2. Johnson M et al (2015) Team ihmc's lessons learned from the darpa robotics challenge trials. J Field Robot 32(2):192–208
3. Mason MT, Salisbury JK Jr (1985) Robot hands and the mechanics of manipulation
4. Pratt GA et al (1997) Stiffness isn't everything. In: Khatib O, Salisbury JK (eds) Experimental robotics IV. LNCIS. Springer, Berlin, pp 253–262
5. Kimura H, Fukuoka Y (2004) Biologically inspired adaptive dynamic walking in outdoor environment using a self-contained quadruped robot: 'tekken2'. In: Proceedings of 2004 IEEE/RSJ international conference on intelligent robots and systems (IROS 2004), vol 1. IEEE, pp 986–991
6. Malzahn J (2014) Modeling and control of multi-elastic-link robots under gravity: from oscillation damping and position control to physical interaction. VDI
7. Howell LL (2001) Compliant mechanisms. Wiley, Hoboken
8. D'Imperio M et al (2014) Modelling legged robot multi-body dynamics using hierarchical virtual prototype design. Lecture Notes in Computer Science (LNAI), vol 8608, pp 59–71
9. D'Imperio M et al (2015) Dynamic analysis using numerical multi-body approach for quadruped robots. In: Thematic conference on multibody dynamics ECCOMAS. IEEE
10. Chase RP Jr et al (2011) A 3-d chain algorithm with pseudo-rigid-body model elements. Mech Based Des Struct Mach 39(1):142–156
11. Howell LL (1991) The design and analysis of large-deflection members in compliant mechanisms. PhD dissertation
12. Semini C (2010) HyQDesign and development of a hydraulically actuated quadruped robot. Doctor of Philosophy (PhD), University of Genoa, Italy